JOURNAL OF SOLID STATE CHEMISTRY 103, 314–321 (1993)

Tl^+ Ion Conductivity in $Rb_xTl_{(1-x)}I$ for $0 \leq x \leq 0.10$, Coexistence of Mixed Phases, and Phase Stabilization

PENG-NIAN HUANG* AND E. A. SECCO†

Chemistry Department, St. Francis Xavier University, Antigonish, Nova Scotia, Canada B2G 1C0

Received January 16, 1992; in revised form August 21, 1992; accepted August 25, 1992

The ac electrical conductivity versus temperature dependence of $Rb_xTl_{(1-x)}I$ for $0 \leq x \leq 0.10$ is reported. The solid–solid phase transition (yellow) β-TlI $\rightleftarrows$ (red) α-TlI occurs at 172°C with transition enthalpy $\Delta H_t = 865$ J/mole and is accompanied by a sharp jump in conductivity, ca. two orders of magnitude. The reverse $\alpha \rightarrow \beta$ transition exhibits a distinct hysteresis dependent on pressure and rate of cooling. The high conductivity α-phase can be obtained at room temperature (i) by application of pressure to the β-solid, (ii) by rapid quenching of the melt, and (iii) by incorporating 5–9 mole% RbI in TlI lattice. The conductivity data and Q_c values, while sensitive to sample history and pretreatment, show reproducible behavior. The observed Q_c(eV) values are 0.39 ± 0.04 for the cool mode of compressed α- and β-TlI and the heat mode of $Rb_{0.05}Tl_{0.95}I$, 0.50–0.62 for all α-TlI samples and $Rb_{0.10}Tl_{0.90}I$, and 0.64–0.97 for all β-TlI samples prior to the β–α transition. No solid–solid phase transition is observed for RbI and its conductivity is lower than that of TlI by a factor of 10^5 at ~175°C. The mechanism and structure interpretations of these results are presented.

Introduction

Solid state fast ion conductors, characterized by very high ionic conductivity relative to most ionic solids which in some cases exceeds the ionic conductivity in the liquid phase, have attracted much attention recently. Studies on these conductors focus on an understanding of the factors directly affecting the mobility of the ions and the mechanism of ion transport with the expectation of incorporating these compounds for use in various electrochemical devices.

A number of ionic solids undergo solid phase transitions to a high temperature phase accompanied by a sharp jump in ionic conductivity. There is a qualitative resemblance of the logarithm conductivity (σT) versus T^{-1} plot for these solids, e.g., alkali sulfates, Ag_2SO_4, Tl_2SO_4, AgI, Li_2MCl_4 spinels, to the site percolation probability function, i.e., the $P(p)$ plot (*1*, *2*), suggesting the percolation model for ion transport. The P versus p curve describes the function $P(p)$, where P is the percolation probability or the fraction of the system taken up by the percolation path and p represents the probability that a site is unblocked or the probability of intersite connectivity to an activated hopping ion. That is, at the phase transition or the percolation threshold the number of intersite channel connectivities or the percolation probability in the network structure increases sharply, giving rise to the ob-

* Shanghai Institute of Ceramics, Academia Sinica, Shanghai, People's Republic of China.

† To whom correspondence should be addressed.

0022-4596/93 $5.00

served sudden jump in ion conductivity. Fast-ion conduction in solids is considered a paradigm for a structure–property relation, where the ionic conductivity σ is a composite quantity $\sigma = nq\mu$ with n the charge carrier concentration, q the carrier charge, and μ the mobility of the carriers. The carrier mobility is related to a set of energetically favorable sites that are not normally occupied. The concomitant volume expansion for the sulfates, i.e., $+\Delta V$ of 3–4.5%, with the phase transition implies, *ceteris paribus,* that structure "free" volume was a major contributing factor to conductivity enhancement in these comounds (*3–5*) and in the lower density glass phase relative to crystal for Na^+, Cu^+ and Li^+ ion conductivity compositions (*6–8*). The conductivity jump-free volume correlation is, however, not observed for AgI, TlI, and CsCl, where the structure factor overrides the volume factor. In AgI and TlI the phase transition is accompanied by a volume decrease where the structure undergoes a change from shared corners and/or edges of coordination polyhedra to shared faces, resulting in a significant increase in the number of accessible/occupancy sites for the mobile ion with lower activation energy. Furthermore, recent studies incorporating quasi-equal radius Rb^+ (166 pm) and Tl^+ (164 pm) in Ag_2SO_4 failed to support the conductivity–free volume relationship in sulfates (*9, 10*). Also, the ionic conductivity of Tl_2SO_4, $\sim 10^3$ higher than Rb_2SO_4, is of the same order of magnitude as that of Ag_2SO_4 (*10*) despite the larger mass of Tl^+ (factor of 2) and the larger Tl^+ radius, viz. $r_{Tl^+} = 164$ pm vs $r_{Ag^+} = 129$ pm for CN = 6 (*11*). These inconsistencies point to factors other than the geometry of the anion array and structure "free" volume as major contributors to ionic conductivity, such as the bonding characteristics of the mobile cation (*12*).

Since the chemistry of Tl^+ bears some resemblance to that of Ag^+ (*13*) with differences linked to the lone electron pair, Ag^+-$4d^{10}$ versus Tl^+-$5d^{10}6s^2$, TlI was chosen along with RbI for a parallel study with AgI to be compared with Tl_2SO_4 and Ag_2SO_4. Yellow TlI transforms at 175°C to a red cubic form; i.e., (yellow) β-TlI $\rightleftarrows$ (red) α-TlI which is accompanied by 3% reduction in volume paralleling the decrease in volume of 6% for AgI at its phase transition 147°C. Yellow β-TlI is a double layered orthorhombic structure related to NaCl. The structure of α-TlI is a $Pm3m$ CsCl-type in common with the room-temperature-stable structure of its analogs TlCl and TlBr. The conductivity study on single crystal TlI (*14*) reported a jump at its transition along with the unusual behavior of higher activation energy for the high temperature α-phase than for the low temperature β-phase. The presence of 20 mole% Rb^+ in AgI in the form of the compound $RbAg_4I_5$ resembles α-AgI by exhibiting high conductivity at room temperature. The composition RbI:4TlI showed a constant melting temperature interpreted as $RbTl_4I_5$ in the early stage of our study. These results prompted us to investigate the effect of Rb^+ in TlI with the similar aim of stabilizing or preserving the high conductivity phase of TlI.

Experimental

The RbI and TlI used in this work were obtained from Aldrich Chemical Corp. with stated purity 99.9% and 99.999%, respectively. The samples studied were prepared by grinding the requisite compositions in a mortar and were fused in a Pyrex container in a well-type furnace maintained at ~50 K above the melting temperature under atmospheric conditions for a half hour. Since the RbI–TlI condensed phase diagram was not available until after completion of the study (*15*) the melting temperature was determined visually or by thermal analysis. The solid was obtained (i) by pouring the melt immediately into a stainless steel mold, i.e., rapid quenching, or (ii) by allowing the sam-

ple to remain in the furnace overnight after cutting of the power, i.e., slow cooling. Spot checks on after-melted sample weights showed neglible weight loss ~0.01%, indicating that the sample maintained the composition of its original components.

The ac electrical conductivity measurements were done on both compressed and uncompressed solidifed fused mass samples using the two terminal method described earlier (*16, 6*). All samples were ca. 13 mm diameter and 2 mm thick; compressed samples were prepared under a pressure of 10 MPa for 15 min. Both surfaces of the sample were touched with graphite (DAG #154 Acheson) to ensure proper contact. The sample was maintained by a spring-loaded support between stainless steel leads using two polished Pt discs as electrodes. The conductivity was measured under reduced pressure (~10^{-3} Torr) with a GenRad 1688 LC Digibridge interfaced to an Apple IIe microcomputer and Epson PX-85 printer at 1 kHz at heating and cooling rate of ~1° min^{-1} except where otherwise specified. Temperature was monitored by standardized chromel–alumel thermocouple with a Hewlett–Packard 3478A Multimeter. Our conductivity technique has been confirmed on two $Ag/RbSO_4$ sample compositions with σ values in the same conductivity range in an argon atmosphere over the frequency 0.1–10.0 kHz in 10 Hz intervals by a more sophisticated impedance setup in an independent laboratory (*17*). While it is possible that at a frequency of 1 kHz electrode polarization contributes to measured σ values our confidence rests on the very good agreement between our σ values and those of previous workers using different measurement techniques in independent laboratories (*14, 18–20*).

The differential scanning calorimetry (DSC) traces were recorded on a DuPont 1090B Thermal Analyzer equipped with disk memory and data analyzer. Measurements were made in a flowing N_2 (ultrapure) atmosphere using a gold pan as reference. The samples were encapsulated in gold pans. The calorimeter was calibrated using the enthalpy of fusion for In metal before the transition enthalpies of $Rb_xTl_{(1-x)}I$ were determined.

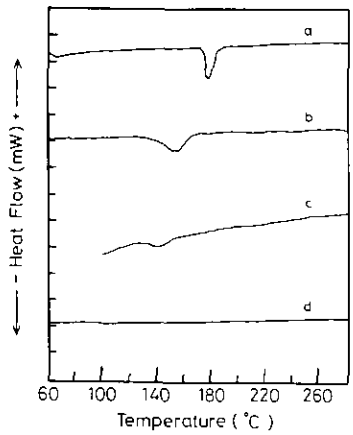

FIG. 1. Differential scanning calorimetry (DSC) heating traces for $Rb_xTl_{(1-x)}I$: (a) $x = 0$, (b) $x = 0.025$, (c) $x = 0.035$, (d) $x = 0.05$.

Results and Discussion

The $\beta \rightleftarrows \alpha$ phase transition in pure TlI occurs at 172°C, Fig. 1, with the transition enthalpy $\Delta H_t = 865$ J/mole. The transition temperature is in good agreement with the reported values of 170–175°C (*14, 22*). The incorporation of up to 5 mole% RbI in TlI shifts the transition to lower temperature with reduced ΔH_t which eventually falls to zero. The dependence of ΔH_t on mole fraction of RbI is given in Fig. 2, where the dashed curve represents expected dependence calculated for fractions of β-TlI in $Rb_xTl_{(1-x)}I$ taking $\Delta H_t = 865$ J/mole and zero for $x = 0$ and 0.05, respectively. The composition of $Rb_{0.05}Tl_{0.95}I$ is red in color with no transition endotherm on DSC trace, suggesting that the high temperature α-TlI is preserved at room temperature. Confirmatory structural evidence for the α-phase

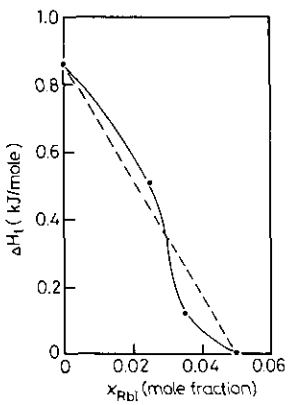

FIG. 2. Enthalpy of transition versus mole fraction RbI: (———) calculated and (—·—) experimental values.

was obtained from X-ray diffraction spectrum. It is to be noted that the X-ray beam effected a partial conversion to the β-phase, resulting in a mixed orthorhombic–cubic pattern and a mustard yellow product after radiation.

The dependence of the ionic conductivity on temperature usually follows the Arrhenius-type expression

$$\sigma = (nq^2\lambda^2\nu\lambda/kT)\exp(-\Delta G\ddagger/kT), \quad (1)$$

where ν is the jump frequency, λ the intersite distance, γ the intersite geometric constant, k the fundamental constant, and $\Delta G\ddagger$ the free energy of activation. The equation is given in simpler form as

$$\sigma T = \sigma_0' \cdot \exp(-Q_c/RT), \quad (2)$$

where $\sigma_0' = \sigma_0 \exp(\Delta S\ddagger/R)$ and $\Delta H\ddagger = Q_c$, i.e., the activation enthalpy equals the experimental activation energy or the apparent activation energy for mobility, which may include a defect formation enthalpy contribution.

On the basis of Eq. (2), heat and cool mode plots of $\log \sigma T$ versus $T(\mathrm{K})^{-1}$ for various samples of $Rb_xTl_{(1-x)}I$ for different pretreatments, along with Q_c for specific regions, are presented in Figs 3–5. Figure 3 shows conductivity data with jump $>10^2$ on heating for compressed annealed pure TlI, consistent with the single crystal behavior (*14*) and the effect of cooling rate on the hysteresis of $\alpha \rightleftarrows \beta$ transformation. That is, the faster cooling rate extends the hysteresis effect and the lifetime of the α-phase as might be expected from kinetics, i.e., nucleation and growth processes, and strain energies as presented earlier (*3, 21*). The $\beta \rightarrow \alpha$ conductivity jump occurs on heating at 174°C in agreement with the DSC and literature values. The high conductivity α-phase is accompanied by a decrease in activation energy Q_c value.

Figure 4 shows $\log \sigma T$ versus $T(\mathrm{K})^{-1}$ plots for two samples of pure TlI, compressed and unannealed slow cooled (a) and uncompressed unannealed quenched solidified fused mass (b). Both samples exhibited the bright red color at room temperature characteristic of the α-phase. The conductivity behavior, in contrast to the annealed sample in Fig. 3, indicates a nonequilibrated metastable mixed state of α- and β-phases. The unusual behavior of conductivity rise followed by a drop in conductivity on heating, Fig. 4(a), may be explained by a mixed or new phase structure stabilized by pressure. The structure breaks down slowly at ~95°C,

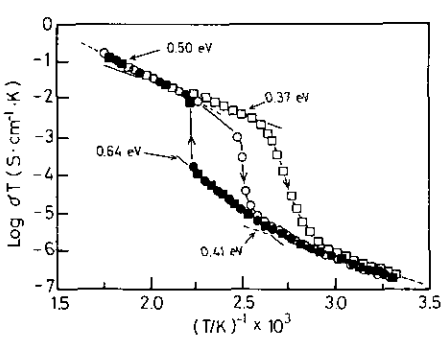

FIG. 3. Plots of $\log \sigma T$ versus $T(\mathrm{K})^{-1}$ of pure TlI (x = 0) at constant heating rate 1°/min ● and ■ but different cooling rates: ○ – 1°/min, □ – 2°/min.

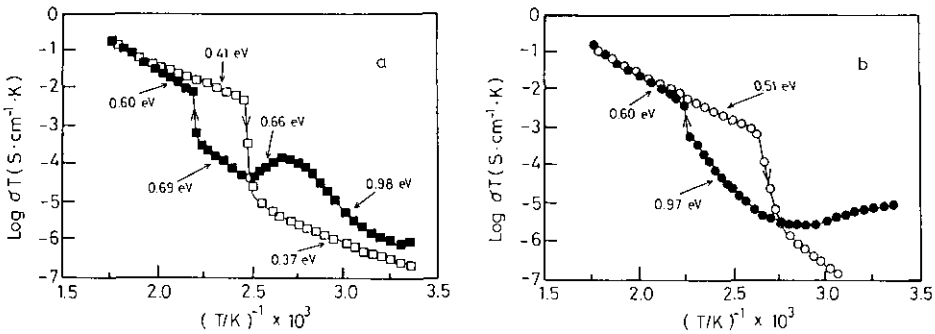

FIG. 4. Plots of log σT versus $T(K)^{-1}$ of pure TlI ($x = 0$): (a) compressed unannealed slow cooled, heating ■, cooling □; (b) uncompressed unannealed quenched solidified fused mass, heating ●, cooling ○.

yielding the stable β-phase prior to the normal $\beta \rightarrow \alpha$ transition. The Q_c value prior to the crossover equals the Q_c prior to the $\beta \rightarrow \alpha$ transition in Fig. 4(b), but the $\beta \rightarrow \alpha$ conductivity jump in Fig. 4(b) is only half that in Fig. 4(a). The structure visualized here parallels the ordered coexistence of mixed phases reported for mixed alkali halide–cyanides (*23*). However, this non-Arrhenius σT behavior at low temperature has been attributed to a different conduction mechanism involving anionic and electronic contributions (*18–20*) or interparticle effect.

A sharp conductivity drop on heating has been reported for other solid phase transitions (*6, 7, 24*). However, the sluggish transformation (second other transition?) of the stable structure to the β-phase in Fig. 4(a) accompanied by a negative temperature dependence equivalent to 0.66 eV suggests two competing energy effects. Taking the simple conductivity process with Q_c of 0.98 eV along with 0.66 eV one obtains an exothermic effect of 1.64 eV. That is, *ceteris paribus*, there is a release of 1.64 eV in the structural rearrangement.

Figure 5 gives the conductivity–temperature dependence for RbI (a), TlI (b), $Rb_{0.10}Tl_{0.90}I$ (c), and $Rb_{0.05}Tl_{0.95}I$ (d) for heat mode only, where each sample was annealed uncompressed quenched solidified fused mass. The effect of annealing is evident for Fig. 5(b) relative to Fig. 4(b). The pertinent features of Fig. 5 include (i) the higher conductivity of TlI relative to RbI by a factor $>10^4$, (ii) the normal conductivity behavior of the β-phase prior to transformation in (b), (iii) the absence of the $\beta \rightarrow \alpha$ conductivity jump in (c) and (d), consistent with the DSC traces, and (iv) the same conductivity for $Rb_{0.05}Tl_{0.95}I$ as for α-TlI in the cool mode for the temperature interval 30–330°C.

Table I shows the relative conductivities at 200°C and the Q_c values of compressed, solidified fused mass, and single crystal TlI along with solidified fused mass $Rb_xTl_{(1-x)}I$ for $x = 0.05$ and 0.10 compositions. The

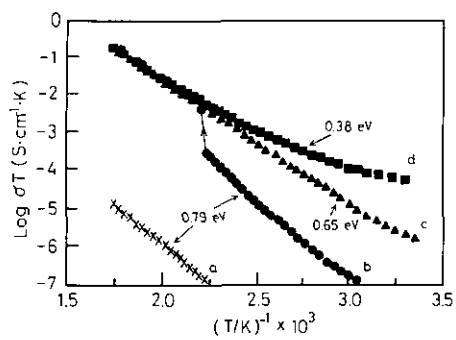

FIG. 5. Plots of log σT versus $T(K)^{-1}$ of (a) RbI, (b) TlI, (c) $Rb_{0.10}Tl_{0.90}I$, (d) $Rb_{0.05}Tl_{0.95}I$.

TABLE I

CONDUCTIVITY AND ACTIVATION ENERGY VALUES FOR $Rb_xTl_{(1-x)}I$

Sample composition	$\sigma_{200°C}$(S · cm^{-1})	α-Q_c(±.04eV)	β-Q_c(±.04eV)
Compressed, annealed, $x = 0$	3.82×10^{-5}	heat—0.50 cool—0.37	heat—0.64 cool—0.41
Solidifed fused bulk, annealed, $x = 0$	2.21×10^{-5}	heat—0.65	heat—0.79
Solidified fused bulk, annealed, $x = 0.05$	2.22×10^{-5}	heat—0.65 0.38	———
Solidified fused bulk, annealed, $x = 0.10$	2.25×10^{-5}	heat—0.65	———
Single crystal, $x = 0$[a]	1.92×10^{-5}	heat—0.73 cool	heat—0.54 cool

[a] Taken from Ref. (*14*).

$\sigma_{200°C}$ values for solidified fused mass TlI, $Rb_xTl_{(1-x)}I$ compositions and single crystal TlI are in excellent agreement but differ from the compressed TlI value by a factor ~2. The striking inverted relationship between our α- and β-phase Q_c values and the single crystal values is evident. Since $Q_c = \Delta H^*_{\text{migration}} + \frac{1}{2}\Delta H_{\text{defect formation}}$, is it reasonable to expect the higher Q_c for single crystal α-TlI at high temperature to contain a defect formation enthalpy contribution as distinct from solidifed fused bulk samples?

Assuming $\beta \rightarrow \alpha$ to be a disorder-type transformation and the conductivity jump to be a disorder related effect, then $\Delta S_t/\Delta \log(\sigma T)_t = 1.2$, suggesting the jump to be almost entirely linked to a disorder effect, which compares with 3.7 for AgI, where disorder is responsible for only 25% of the jump.

The fact that the presence of 5 mole% Rb^+ preserves the high temperature α-phase TlI to room temperature can provide a clue to the mechanism of phase transformation and phase stabilization. Two possible effects responsible for locking in the α-phase suggest themselves: (i) a physical volume effect and (ii) a chemical ion–ion interaction effect. A physical volume effect is ruled out because Rb^+ with ionic radius 166 pm substituting for Tl^+ with ionic radius 164 pm on the Tl^+ sublattice contributes a volume increase to the structure, whereas the $\beta \rightarrow \alpha$ transition is accompanied by a ~3% volume decrease. That is, the increased physical volume would favor the reverse phase direction, viz., $\alpha \rightarrow \beta$. We note the double layered orthorhombic structure related to NaCl for β-TlI to be only slightly removed energetically, i.e., 865 J/mole, from the $Pm3m$ CsCl structure of α-TlI, in common with the room temperature structure of TlCl and TlBr. From simple ion–ion interaction considerations involving the outer electron configuration of Rb^+, i.e., $3d^{10}4s^2p^6$ relative to Tl^+, i.e., $4f^{14}5d^{10}6s^2$, we can visualize bonding between the more electropositive Rb^+ and I^- to be stronger than that between Tl^+ and I^- in the solid. This stronger bonding, paralleling that of TlCl and TlBr, can effect a structural contraction sufficient to stabilize the high temperature α-phase CsCl-type structure of TlI. The situation can be summarized by saying that positive pressure, external or "chemical," increases the existence range of the α-phase as was suggested for the alkali halide–cyanides by Loidl *et al.* (*23*). One can assign 865 J to the phase stabilization energy effected by the presence of 5 mole% Rb^+. This interpretation

can be extended to calculate the differential heat of solution dq/dn of RbI in TlI as ~17 kJ/mole.

Because the logarithm σT versus T^{-1} plot in a solid–solid phase transition resembles the site percolation probability function, i.e., $P(p)$, plot as stated earlier we interpret the ionic conductivity mechanism to be a percolation-type transport mechanism. For phase transitions accompanied by a volume increase, $+\Delta V$, interpretation was focused on structure "free" volume as the major contributing factor in the enhancement of ionic conductivity. However, as in the cases of AgI and TlI, where the phase transition involves a volume decrease, the accessibility of the activated mobile ion to an increased number of interconnecting sites takes precedence over the decrease in volume. The accessibility to interconnecting sites, i.e., between adjacent equilibrium positions, can be governed by the "window-size" relative to the size of the migrating ion and lattice resiliency as indicated by migration or activation volume, along with subtle effects of bond characteristics and framework geometry (*12*). In brief, the maximum solid state ionic conductivity is expected for a high concentration of mobile charge carriers n in the structure with a large number of easily accessible occupancy sites.

Acknowledgments

This study was supported in part by the Natural Sciences and Engineering Research Council of Canada and in part by the University Council for Research. The authors express their gratitude to the referee and to Professor J. M. Honig for helpful and constructive comments and to Dr. Richard A. Secco, University of Western Ontario for the X-ray diffraction spectra.

Note added in proof. The stability of α-$Rb_{0.05}Tl_{0.95}I$ was checked 100 days after its preparation. The DSC trace showed a broad shallow endotherm extending from 127°C to 162°C similar to Fig. 1c with ΔH_t = 740 J/mole. The log σT versus T^{-1} plot parallels that of Fig. 3 for fast cooling with hysteresis extending to 70°C. This suggests α-$Rb_{0.05}Tl_{0.95}I$ to be a metastable state undergoing relaxation. More recent results indicate that the $\alpha \rightarrow \beta$ relaxation begins after 3 days of preparation. A kinetic study of this relaxation is being planned.

References

1. J. M. ZIMAN, "Models of Disorder," Chap. 9, Cambridge Univ. Press, Cambridge (1979).
2. R. ZALLEN, "The Physics of Amorphous Solids," Chap. 4, Wiley, New York (1983).
3. M. S. KUMARI AND E. A. SECCO, *Can. J. Chem.* **61,** 599, 2804 (1983).
4. M. D. LEBLANC, U. M. GUNDUSHARMA, AND E. A. SECCO, *Solid State Ionics* **20,** 61 (1986).
5. E. A. SECCO, *Solid State Commun.* **66,** 921 (1988).
6. U. M. GUNDUSHARMA AND E. A. SECCO, *Appl. Phys. A* **51,** 7 (1990).
7. T. MINAMI AND N. MACHIDA, *in* "Solid State Ionics of International Conference on Advanced Materials—91" (M. Balkanski, T. Takahashi, and H. L. Tuller, Ed.), p. 91, Amsterdam (1992).
8. C. A. ANGELL, *Solid State Ionics*, **9/10,** 3 (1983); **18/19,** 72 (1986).
9. YANJIA LU AND E. A. SECCO, *in* "Proceedings, 8th International Conference Solid State Ionics, Lake Louise, Canada, Oct. 20–26, 1991," in press.
10. YANJIA LU, M. SC. THESIS, St. Francis Xavier University, to be published.
11. R. D. SHANNON, *Acta Crystallogr. Sect. A* **32,** 751 (1976).
12. B. J. WUENSCH, *in* "Solid State Ionics of International Conference on Advanced Materials—91" (M. Balkanski, T. Takahashi, and H. L. Tuller, Eds.), p. 291, Elsevier, Amsterdam (1992).
13. F. A. COTTON AND G. WILKINSON, "Advanced Inorganic Chemistry," 3rd ed., p. 280, Interscience, New York (1972).
14. Z. MORLIN, *Phys. Status Solidi A* **8,** 565 (1971).
15. V. A. ISAENKO AND A. N. KIRGINTSEV, *Zh. Neorg. Khim.* **21** (9), 2581 (1976); *Russ J. Inorg. Chem. (Engl. Transl.)* **21** (9), 1420 (1976); *in* "Phase Diagrams for Ceramists" (L. P. Cook and H. F. McMurdie, Eds.), Vol. 7, No. 7707, Am. Ceram. Soc., Columbus, OH (1989).
16. M. NATARAJAN AND E. A. SECCO, *Can. J. Chem.* **52,** 712 (1974).
17. A. AHMAD, Canada Centre for Mineral and Energy Technology, Ottawa, Ontario, Canada, personal communication.
18. J. W. BRIGHTWELL, L. S. MILLER, A. MUNDAY, AND B. RAY, *Phys. Status Solidi A* **79,** 293 (1983).
19. G. A. SAMARA, *Phys. Rev. B* **23,** 575 (1981).
20. A. SCHIRALDI, A. MAGISTRIS, AND E. PEZZATI, *Z. Naturforsch.* **29,** 782 (1974).

21. K. J. RAO AND C. N. R. RAO, *J. Materials Sci.* **1,** 238 (1966).
22. N. N. GREENWOOD AND A. EARNSHAW, "Chemistry of the Elements," p. 272, Pergamon, New York (1984).
23. E. CIVERA GARCIA, K. KNORR, A. LOIDL, AND S. HAUSSÜHL, *Phys. Rev. B* **36,** 8517 (1987).
24. K. G. MACDONALD, C. MACLEAN, AND E. A. SECCO, *Can. J. Chem.* **66,** 3132 (1988).